



## Antifungal saponins from bulbs of white onion, *Allium cepa* L.

Virginia Lanzotti<sup>a,\*</sup>, Adriana Romano<sup>b</sup>, Stefania Lanzuise<sup>b</sup>, Giuliano Bonanomi<sup>b</sup>, Felice Scala<sup>b</sup>

<sup>a</sup> Dipartimento di Scienza degli Alimenti Università degli Studi di Napoli Federico II, via Università 100, 80055 Portici, Napoli, Italy

<sup>b</sup> Dipartimento di Arboricoltura, Botanica e Patologia vegetale, Università degli Studi di Napoli Federico II, via Università 100, 80055 Portici, Napoli, Italy

### ARTICLE INFO

#### Article history:

Received 27 July 2011

Received in revised form 7 October 2011

Available online 12 December 2011

#### Keywords:

*Allium*

Onion

Saponins

Furostanol-type

Ceposides

Antifungal activity

Structure–activity relationships

### ABSTRACT

Three saponins, named ceposide A, ceposide B, and ceposide C were isolated from the bulbs of white onion, *Allium cepa* L. Elucidation of their structure was carried out by comprehensive spectroscopic analyses, including 2D NMR spectroscopy and mass spectrometry, and chemical evidences. The structures of the compounds were identified as (25R)-furost-5(6)-en-1 $\beta$ ,3 $\beta$ ,22 $\alpha$ ,26-tetraol 1-O- $\beta$ -D-xylopyranosyl 26-O- $\alpha$ -D-rhamnopyranosyl-(1  $\rightarrow$  2)-O- $\beta$ -D-galactopyranoside (ceposide A), (25R)-furost-5(6)-en-1 $\beta$ ,3 $\beta$ ,22 $\alpha$ ,26-tetraol 1-O- $\beta$ -D-xylopyranosyl 26-O- $\alpha$ -D-rhamnopyranosyl-(1  $\rightarrow$  2)-O- $\beta$ -D-glucopyranoside (ceposide B), and (25R)-furost-5(6)-en-1 $\beta$ ,3 $\beta$ ,22 $\alpha$ ,26-tetraol 1-O- $\beta$ -D-galactopyranosyl 26-O- $\alpha$ -D-rhamnopyranosyl-(1  $\rightarrow$  2)-O- $\beta$ -D-galactopyranoside (ceposide C). The isolated compounds, alone and in combinations, were evaluated for their antimicrobial activity on ten fungal species. Antifungal activity of all three saponins increased with their concentration and varied with the following rank: ceposide B > ceposide A–ceposide C. We found a significant synergism in the antifungal activity of the three ceposides against *Botrytis cinerea* and *Trichoderma atroviride*, because growth of these fungi was strongly inhibited when the three saponins were applied in combination. In contrast, *Fusarium oxysporum* f. sp. *lycopersici*, *Sclerotium cepivorum* and *Rhizoctonia solani* were very little affected by saponins.

© 2011 Elsevier Ltd. All rights reserved.

### 1. Introduction

Plants during their life cycles interact with a vast range of different microbial species, including pathogens. Thousands of diverse natural products are produced by plants and many of these are involved in plant defense. The phytochemical diversity of antimicrobial compounds include terpenoids, phenolics, phenylpropanoids, stilbenes, alkaloids, glucosinolates, indole and saponins (Dixon, 2001).

Saponins are a major family of secondary metabolites that occur in a wide range of plant species (Osborn, 1996). Their name comes from the Latin “sapo”, meaning soap and plant material containing saponins were long used for cleaning clothes. Saponins are glycosides with triterpenoid or steroidal aglycone. Triterpene saponins are widely distributed in nature and typical constituents of dicotyledonous, while steroidal saponins are less distributed and usually found in many monocotyledonous families, especially Dioscoreaceae, Agavaceae and Liliaceae. *Allium* plants belong to this last family and are known to possess steroidal saponins (Lanzotti, 2006). Saponins are compounds with a marked antimicrobial activity, and commonly are classified as phytoanticipins because are present in the plant tissue before pathogens’ attack (VanEtten et al., 1994). Their antifungal activity is due to the ability to form complexes

with sterols and results in an increase of fungal membrane permeability and leakage of cell contents (Morrissey and Osborn, 1999). Previous studies showed that plant species belonging to the *Allium* genus are rich in saponins with antifungal activity (Lanzotti, 2005; Barile et al., 2006). Despite the fact that different antimicrobial natural compounds usually occur together within plant tissues, most studies report only the antifungal activity of single molecules. However, it should be pointed out that the toxicity of antimicrobial molecules can be enhanced synergically when they work in combination (Wittstock and Gershenzon, 2002). For instance, Segura et al. (1999) reported that the peptide snaking-1 act synergically with the defensin PTH1 against the bacteria *Clavibacter michiganensis* subsp. *Sepedonicus*. Lorito et al. (1994) found that mixtures of cell wall degrading enzymes and fungitoxic compounds synergistically enhanced the antifungal properties against *Botrytis cinerea*. Concerning saponins, a recent study (De Lucca et al., 2006) observed synergistic activity between CAY-1, a saponin from *Capsicum frutescens*, and amphotericin B, a polyene antifungal drug, against a variety of fungal species.

In our work on the discovery of bioactive saponins from *Allium* species (Lanzotti, 2005), we examined white onion, *Allium cepa* L. This species is a cultivated perennial plant used for food preparation. We isolated and determined the structure of three new furostanol saponins, named ceposides A–C (1–3). The stereostructure of these compounds was elucidated by extensive NMR techniques and chemical methods. Moreover, we assessed the effects

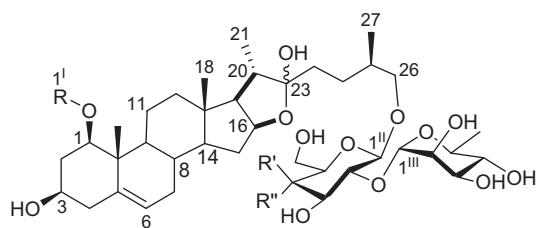
\* Corresponding author. Tel.: +39 081 2539459; fax: +39 081 7754942.

E-mail address: [lanzotti@unina.it](mailto:lanzotti@unina.it) (V. Lanzotti).

of the three novel saponins, alone and in combination, on a wide range of fungal species to evaluate their possible involvement in *A. cepa* resistance to pathogens' attack.

## 2. Results and discussion

Fresh bulbs of white onion, *A. cepa* L., were extracted with acetone, following a procedure described in Lanzotti, 2006. The use of acetone, as reported previously (Corea et al., 2003), avoid the formation of 22-O-methyl derivatives of furostanol saponins, which are artifacts formed during the extraction procedure with MeOH. The obtained organic acetone extract was taken to dryness and then partitioned between EtOAc, butanol and water. The butanol-soluble portion, by TLC (SiO<sub>2</sub>, butanol/acetic acid/water



Ceposide A (1) R = β-D-Xyl R<sup>I</sup>=OH R<sup>II</sup>=H

Ceposide B (2) R = β-D-Xyl R<sup>I</sup>=H R<sup>II</sup>=OH

Ceposide C (3) R = β-D-Gal R<sup>I</sup>=OH R<sup>II</sup>=H

**Chart 1.** Chemical structures of ceposide A (1), ceposide B (2), and ceposide C (3).

60:15:25, v/v/v) was shown to contain saponins, first separated by MPLC, obtaining a crude saponin fraction (18 mg kg<sup>-1</sup> fresh wt). This was further purified by HPLC techniques, affording the new compounds ceposide A (1, 9.8 mg kg<sup>-1</sup> fresh wt), B (2, 3.0 mg kg<sup>-1</sup>), and C (3, 2.1 mg kg<sup>-1</sup>), together with ascalonicoside A (1.4 mg kg<sup>-1</sup>), previously isolates from *Allium ascalonicum* (Fattorusso et al., 2002).

Ceposide A (1, Chart 1), isolated as an amorphous solid, was the most abundant compound in saponin fraction. Its negative HRFAB MS spectrum gave a pseudomolecular ion peak at *m/z* 887.4632 (M-H)<sup>-</sup>, which together with <sup>13</sup>C NMR data suggested the molecular formula as C<sub>44</sub>H<sub>72</sub>O<sub>18</sub>. Preliminary <sup>1</sup>H NMR analysis of 1 (CD<sub>3</sub>OD, Tables 1 and 3) showed five methyl groups (two singlet and three doublets), some overlapping signals between δ 1.1 and 2.6, and a number of signals from δ 3.2 and 5.6. This series of signals suggested a saponin nature of the compound. A characteristic hemiacetal signal at δ 113.0 in <sup>13</sup>C NMR spectrum (Table 2) indicated its furostanol nature, while the presence of Δ<sub>5</sub> unsaturation has been suggested by a signal at δ 5.57 (bd, *J* = 3.2 Hz) in the <sup>1</sup>H NMR of 1, attributed to H-6. <sup>13</sup>C NMR spectrum of 1 (Table 3) also showed three anomeric carbon signals at δ 101.2, 102.5, and 104.3, indicating the presence of three saccharide residues.

Combined analysis of 2D COSY and HOHAHA spectra of 1 allowed to detect five spin systems, two belonging to the aglycone moiety, and the remaining three to three sugars. Consequently, each proton has been related to the directly bonded carbon through a HSQC spectrum.

Concerning the aglycone, the first spin system started from ring A and extended up to ring E protons, while the second spin system included the side chain protons (C-23 to C-27). The HMBC cross-peaks, reported in Fig. 1, allowed to connect the two spin systems

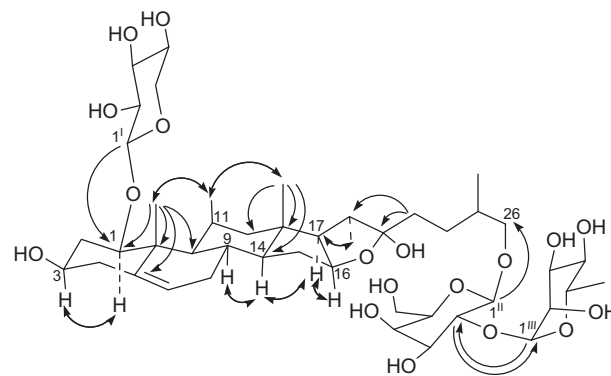
**Table 1**  
<sup>1</sup>H NMR data of the Aglycone Portions of Ceposide A (1), B (2), and C (3) 500 MHz, CD<sub>3</sub>OD.

Position	1 δ <sub>H</sub> (int., mult., <i>J</i> in Hz)	2 δ <sub>H</sub> (int., mult., <i>J</i> in Hz)	3 δ <sub>H</sub> (int., mult., <i>J</i> in Hz)
1	3.35 <sup>a</sup>	3.36 <sup>a</sup>	3.35 <sup>a</sup>
2a	2.15 <sup>a</sup>	2.08 <sup>a</sup>	2.13 <sup>a</sup>
b	1.67 <sup>a</sup>	1.66 <sup>a</sup>	1.65 <sup>a</sup>
3	3.34 <sup>a</sup>	3.31 <sup>a</sup>	3.34 <sup>a</sup>
4a	2.21 (1H, dd, 11.5, 7.3)	2.20 (1H, dd, 11.5, 7.3)	2.21 (1H, dd, 11.5, 7.3)
b	2.18 (1H, dd, 11.5, 3.5)	2.16 (1H, dd, 11.5, 3.5)	2.17 (1H, dd, 11.5, 3.5)
6	5.57 (1H, bd, 3.2)	5.59 (1H, bd, 3.2)	5.57 (1H, bd, 3.2)
7a	1.96 <sup>a</sup>	1.95 <sup>a</sup>	1.95 <sup>a</sup>
b	1.95 <sup>a</sup>	1.94 <sup>a</sup>	1.95 <sup>a</sup>
8	1.50 (1H, m)	1.50 (1H, m)	1.50 (1H, m)
9	1.23 <sup>a</sup>	1.28 <sup>a</sup>	1.24 <sup>a</sup>
11a	2.57 (1H, dd, 10.5, 2.5)	2.55 (1H, dd, 10.5, 2.5)	2.57 (1H, dd, 10.5, 2.5)
b	1.45 (1H, m)	1.43 (1H, m)	1.45 (1H, m)
12a	1.70 <sup>a</sup>	1.71 <sup>a</sup>	1.70 <sup>a</sup>
b	1.22 <sup>a</sup>	1.20 <sup>a</sup>	1.20 <sup>a</sup>
14	1.23 (1H, m)	1.23 (1H, m)	1.22 (1H, m)
15a	1.94 <sup>a</sup>	1.94 <sup>a</sup>	1.92 <sup>a</sup>
b	1.24 <sup>a</sup>	1.30 <sup>a</sup>	1.26 <sup>a</sup>
16	4.38 (1H, q, 5.5)	4.38 (1H, q, 5.5)	4.38 (1H, q, 5.5)
17	1.71 <sup>a</sup>	1.71 <sup>a</sup>	1.71 <sup>a</sup>
18	0.81 (3H, s)	0.84 (3H, s)	0.81 (3H, s)
19	1.09 (3H, s)	1.09 (3H, s)	1.10 (3H, s)
20	2.15 <sup>a</sup>	2.15 <sup>a</sup>	2.15 <sup>a</sup>
21	0.98 (3H, d, 6.6)	1.00 (3H, d, 6.6)	0.98 (3H, d, 6.6)
23a	1.74 <sup>a</sup>	1.75 <sup>a</sup>	1.74 <sup>a</sup>
b	1.65 <sup>a</sup>	1.67 <sup>a</sup>	1.65 <sup>a</sup>
24a	1.49 <sup>a</sup>	1.50 <sup>a</sup>	1.49 <sup>a</sup>
b	1.22 <sup>a</sup>	1.30 <sup>a</sup>	1.22 <sup>a</sup>
25	1.73 (1H, m)	1.78 (1H, m)	1.75 (1H, m)
26a	3.80 (1H, dd, 8.5, 6.9)	3.79 (1H, dd, 8.5, 6.9)	3.81 (1H, dd, 8.5, 6.9)
b	3.34 <sup>a</sup>	3.34 <sup>a</sup>	3.31 <sup>a</sup>
27	0.95 (3H, d, 6.6)	0.96 (3H, d, 6.6)	0.95 (3H, d, 6.6)

<sup>a</sup> Overlapped with other signals.

**Table 2**  
<sup>13</sup>C NMR data of the Aglycone Portion of **1**, **2**, and **3** [125 MHz, CD<sub>3</sub>OD].

Position	<b>1</b> δ <sub>c</sub> (mult.)	<b>2</b> δ <sub>c</sub> (mult.)	<b>3</b> δ <sub>c</sub> (mult.)
1	83.2 (CH)	83.5 (CH)	83.7 (CH)
2	39.9 (CH <sub>2</sub> )	39.9 (CH <sub>2</sub> )	39.8 (CH <sub>2</sub> )
3	67.6 (CH)	67.6 (CH)	67.5 (CH)
4	42.0 (CH <sub>2</sub> )	42.0 (CH <sub>2</sub> )	42.1 (CH <sub>2</sub> )
5	138.8 (C)	138.4 (C)	138.8 (C)
6	124.6 (CH)	124.9 (CH)	124.7 (CH)
7	31.6 (CH <sub>2</sub> )	31.5 (CH <sub>2</sub> )	31.6 (CH <sub>2</sub> )
8	33.0 (CH)	32.9 (CH)	33.0 (CH)
9	50.0 (CH)	50.3 (CH)	50.1 (CH)
10	42.2 (C)	42.4 (C)	42.1 (C)
11	24.9 (CH <sub>2</sub> )	24.9 (CH <sub>2</sub> )	24.9 (CH <sub>2</sub> )
12	40.8 (CH <sub>2</sub> )	40.8 (CH <sub>2</sub> )	40.8 (CH <sub>2</sub> )
13	40.5 (C)	40.5 (C)	40.5 (C)
14	57.0 (CH)	56.9 (CH)	57.0 (CH)
15	33.0 (CH <sub>2</sub> )	33.0 (CH <sub>2</sub> )	33.1 (CH <sub>2</sub> )
16	81.2 (CH)	81.3 (CH)	81.2 (CH)
17	64.2 (CH)	64.2 (CH)	64.2 (CH)
18	16.0 (CH <sub>3</sub> )	15.9 (CH <sub>3</sub> )	16.0 (CH <sub>3</sub> )
19	14.5 (CH <sub>3</sub> )	14.4 (CH <sub>3</sub> )	14.5 (CH <sub>3</sub> )
20	40.1 (CH)	40.1 (CH)	40.0 (CH)
21	15.1 (CH <sub>3</sub> )	15.0 (CH <sub>3</sub> )	15.1 (CH <sub>3</sub> )
22	113.0 (C)	112.9 (C)	113.0 (C)
23	36.5 (CH <sub>2</sub> )	36.5 (CH <sub>2</sub> )	36.4 (CH <sub>2</sub> )
24	28.0 (CH <sub>2</sub> )	27.9 (CH <sub>2</sub> )	28.0 (CH <sub>2</sub> )
25	34.1 (CH)	34.0 (CH)	34.1 (CH)
26	74.5 (CH <sub>2</sub> )	75.5 (CH <sub>2</sub> )	74.8 (CH <sub>2</sub> )
27	16.6 (CH <sub>3</sub> )	16.5 (CH <sub>3</sub> )	16.6 (CH <sub>3</sub> )

**Fig. 1.** Selected HMBC (H → C) and ROESY (H ↔ H) correlations exhibited by compound **1**.

through the quaternary C-22 and to build up the structure of the aglycone moiety as furost-5-en-1,3,22,26-tetraol.

The diaxial coupling between H-1 and H-3, detected in a ROESY spectrum (Fig. 1), indicated a *cis* orientation among them and a β-configuration of the hydroxyl at C-3. The 25R stereochemistry of the side chain was deduced by the resonances of protons and carbons at C-25, C-26 and C-27, and by the vicinal couplings between H-25, and the two H-26, in comparison with literature data (Dong

et al., 2001). The following ROESY correlations (Fig. 1), H-11/H<sub>3</sub>-19, H-11/H<sub>3</sub>-18, H-9/H-14, H-14/H-16, H-16/H-17, and H-17/H<sub>3</sub>-21 completed the relative stereochemistry of **1** with the usual B/C *trans*, C/D *trans*, D/E *cis*, and C-20α stereochemistry (Dong et al., 2001; Corea et al., 2005). On the basis of those data, the stereostructure of the aglycone has been determined as depicted in formula. Finally, the stereochemistry at C-22 has been assigned as β by accurate analysis of NMR data, and comparison with other compounds previously described (Corea et al., 2003, 2005; Barile et al., 2007). However, as observed for other furostanol saponins (Corea et al., 2003, 2005), compound **1**, left in aqueous solution overnight at room temperature, gave rise to the equilibrated mixture of the two hemiacetals at C-22 (22α-OH and 22β-OH, 30% and 70% respectively).

Concerning the saccharide portion, the analysis started with the association of the three anomeric protons (δ 4.30, 4.94 and 5.32) with the relevant anomeric carbon signals (δ 101.2, 104.3 and 102.5, respectively), through the HSQC experiment. The nature of the single monosaccharides and their sequence has been

**Table 3**  
<sup>1</sup>H and <sup>13</sup>C NMR data of the Sugar Portion of **1**, **2** and **3** (500 MHz and 125 MHz, CD<sub>3</sub>OD).

Pos.	<b>1</b> δ <sub>H</sub> , int., mult., J in Hz δ <sub>c</sub> (mult.)	<b>2</b> δ <sub>H</sub> (int., mult., J in Hz) δ <sub>c</sub> (mult.)	<b>3</b> δ <sub>H</sub> (int., mult., J in Hz)	δ <sub>c</sub> (mult.)
	Xyl	Xyl	Gal	
1 <sup>I</sup>	4.94 (1H, d, 7.4)	104.3 (CH)	4.32 (1H, d, 7.5)	100.7 (CH)
2 <sup>I</sup>	3.28 <sup>a</sup>	75.7 (CH)	3.71 <sup>a</sup>	74.1 (CH)
3 <sup>I</sup>	3.55 <sup>a</sup>	78.3 (CH)	3.68 (1H, dd, 6.8, 2.5)	75.3 (CH)
4 <sup>I</sup>	3.61 (1H, ddd, 2.1, 7.8, 8.8)	71.8 (CH)	3.87 (1H, dd, 3.2, 2.5)	76.2 (CH)
5 <sup>I a</sup>	3.30 <sup>a</sup>	71.0 (CH <sub>2</sub> )	3.45 <sup>a</sup>	74.1 (CH)
b	3.92 <sup>a</sup>			
6 <sup>I a</sup>			3.47 <sup>a</sup>	62.4 (CH <sub>2</sub> )
b			3.65 <sup>a</sup>	
	Gal	Glc	Gal	
1 <sup>II</sup>	4.30 (1H, d, 7.5)	101.2 (CH)	4.30 (1H, d, 7.5)	101.2 (CH)
2 <sup>II</sup>	3.84 <sup>a</sup>	78.5 (CH)	3.82 <sup>a</sup>	78.5 (CH)
3 <sup>II</sup>	3.62 (1H, dd, 6.8, 2.5)	76.6 (CH)	3.63 (1H, dd, 6.8, 2.5)	76.6 (CH)
4 <sup>II</sup>	3.87 (1H, dd, 3.2, 2.5)	78.2 (CH)	3.87 (1H, dd, 3.2, 2.5)	78.1 (CH)
5 <sup>I a</sup>	3.45 <sup>a</sup>	74.4 (CH)	3.45 <sup>a</sup>	74.4 (CH)
6 <sup>I a</sup>	3.47 <sup>a</sup>	62.5 (CH <sub>2</sub> )	3.47 <sup>a</sup>	62.5 (CH <sub>2</sub> )
b	3.65 <sup>a</sup>		3.65 <sup>a</sup>	
	Rha	Rha	Rha	
1 <sup>III</sup>	5.32 (1H, bs)	102.5 (CH)	5.32 (1H, bs)	102.5 (CH)
2 <sup>III</sup>	3.91 (1H, bs)	72.5 (CH)	3.91 (1H, bs)	72.5 (CH)
3 <sup>III</sup>	3.72 (1H, d, 6.5)	70.5 (CH)	3.72 (1H, d, 6.5)	70.5 (CH)
4 <sup>III</sup>	3.40 (1H, dd, 6.5, 6.0)	72.0 (CH)	3.40 (1H, dd, 6.5, 6.0)	72.0 (CH)
5 <sup>I</sup>	4.11 (1H, dq, 6.6, 6.0)	68.8 (CH)	4.11 (1H, dq, 6.6, 6.0)	68.8 (CH)
6 <sup>I</sup>	1.28 (3H, d, 6.6)	18.2 CH <sub>3</sub> )	1.28 (3H, d, 6.6)	18.2 CH <sub>3</sub> )

<sup>a</sup> Overlapped with other signals.

determined by combined analysis of 2D COSY, HOHAHA, HSQC, and HMBC experiments. Starting from the anomeric proton of each sugar unit, all the proton signals within each spin system were recognized by COSY and HOHAHA spectra, and then connected to the relevant carbon by HSQC spectrum. Then, HMBC and ROESY spectra gave key information on the glycosidic linkages. The data obtained indicated that all sugars were in the pyranose form but they have different nature being hexose, pentose and deoxyhexose. Combined analysis of the coupling constants of each spin system, taken by  $^1\text{H}$  NMR spectrum or by  $^1\text{H}$  sub-spectrum of 2D HOHAHA, together with informations on the spatial proximity of protons obtained by 2D ROESY (e.g. diaxial couplings between  $\text{H}1^{\text{I}}\text{-H}3^{\text{I}}$  and  $\text{H}3^{\text{I}}\text{-H}5^{\text{I}}$ ) allowed the identification of galactose, xylose and rhamnose. Gal and Xyl were determined as  $\beta$ -anomers on the basis of the large  $J_{\text{H}1\text{-H}2}$  coupling constants. Rha were determined as  $\alpha$ -anomer by the small  $J_{\text{H}1\text{-H}2}$  coupling constant and by the chemical shift of  $\text{C}3^{\text{III}}$  and  $\text{C}5^{\text{III}}$  (Corea et al., 2005).

Furthermore, ROESY ( $\text{H}2^{\text{II}}/\text{H}1^{\text{III}}$ ) and HMBC ( $\text{C}2^{\text{II}}/\text{H}1^{\text{III}}$  and  $\text{H}2^{\text{II}}/\text{C}1^{\text{III}}$ ) correlations allowed to get the sequence deduction of a disaccharide chain, composed of  $\beta$ -galactose (residue II) and  $\alpha$ -rhamnose (residue III), that has been placed at C-26 of the aglycone on the basis of the HMBC C-26/ $\text{H}1^{\text{II}}$  correlation. Finally, the remaining  $\beta$ -xylose (residue I) has been located at C-1 by considering the ROESY ( $\text{H}1/\text{H}1^{\text{I}}$ ) and HMBC ( $\text{C}1/\text{H}1^{\text{I}}$  and  $\text{H}1/\text{C}1^{\text{I}}$ ) cross peaks.

To confirm the nature of the sugar units and to determine their absolute configuration, **1** has been subjected to acid hydrolysis (1 N HCl), followed by trimethylsilylation and GC analysis on a chiral column in comparison with both series of galactose, glucose, xylose and rhamnose. By this procedure, we confirmed the nature of sugars and identified their absolute stereochemistry as d. This procedure has been applied to all new isolated compounds. All these data indicated the structure of **1** as (25R)-furost-5(6)-en-1 $\beta$ ,3 $\beta$ ,22 $\alpha$ ,26-tetraol 1-O- $\beta$ -D-xylopyranosyl 26-O- $\alpha$ -D-rhamnopyranosyl-(1  $\rightarrow$  2)-O- $\beta$ -D-galactopyranoside.

Ceposide B (**2**, Chart 1), isolated as an amorphous solid, showed the same molecular formula of **1**. Analysis of 2D NMR spectra of **2** indicated the same aglycone portion. Differences between **1** and **2** were found in the saccharide portion composed by  $\beta$ -Glc,  $\beta$ -Xyl, and  $\alpha$ -Rha. This identification has been obtained both by analysis of 2D NMR spectra of the intact compound and by GC of the hydrolysed compound in comparison with both series of standard sugars. In particular, detailed NMR analyses, including HMBC spectrum, of ceposide B (**2**) in comparison with data of ceposide A (**1**), showed that in **2** one  $\beta$ -Glc residue substitutes the inner  $\beta$ -Gal at C-26 at the same place and connection of **1**. Therefore, the chemical structure of **2** by spectroscopic and chemical evidences has been determined as (25R)-furost-5(6)-en-1 $\beta$ ,3 $\beta$ ,22 $\alpha$ ,26-tetraol 1-O- $\beta$ -D-xylopyranosyl 26-O- $\alpha$ -D-rhamnopyranosyl-(1  $\rightarrow$  2)-O- $\beta$ -D-glucopyranoside.

Ceposide C (**3**), was isolated as an amorphous solid and showed a molecular formula of  $\text{C}_{45}\text{H}_{74}\text{O}_{19}$ , deduced by HRFAB MS and confirmed by  $^{13}\text{C}$  NMR data (Tables 2 and 3). Also in this case, the structure elucidation of ceposide C (**3**) was aided by comparison with the MS and NMR data obtained for ceposide A (**1**) and B (**2**). First of all, the molecular formula of **3** differed from **1** and **2** in being 30 amu higher. The NMR profiles of **3** (Tables 1–3) appeared superimposable with those of **1** and **2** for the signals relative to the aglycone and showed differences in the saccharide nature. Accurate analysis of 2D NMR spectra suggested the presence of the same disaccharide chain of compound **1**, composed of  $\beta$ -galactose and  $\alpha$ -rhamnose. Differences with **1** were related to the third sugar unit, that by MS data appeared based on a hexopyranose structure instead of pentapyranose. Its identification as  $\beta$ -galactose has been obtained by 2D NMR analysis and GC analysis of the hydrolysed

compound. Therefore, the structure of **3** has been identified as (25R)-furost-5(6)-en-1 $\beta$ ,3 $\beta$ ,22 $\alpha$ ,26-tetraol 1-O- $\beta$ -D-galactopyranosyl 26-O- $\alpha$ -D-rhamnopyranosyl-(1  $\rightarrow$  2)-O- $\beta$ -D-galactopyranoside.

Ceposides A–C are characterized by a rare glycosylation at the hydroxyl group on C-1 of the aglycone. This structural feature has been also found for the furostanol saponins named ascalonicosides and tropeosides, previously isolated from the taxonomic related species *A. ascalonicum* (Fattorusso et al., 2002) and *A. cepa* var. *Tropea* (Corea et al., 2005), respectively.

The isolated ceposides, alone and in combinations, were evaluated for their antimicrobial activity on ten fungal species. All three ceposides showed a significant antifungal activity depending on their concentration and the tested fungal species. In general, the saponins showed the following rank of antifungal activity: ceposide B > ceposide A ~ ceposide C (Fig. 2). Saponins differ in the nature of saccharide residues. Ceposide A and B have a Xyl unit (residue I) at C-1 of the aglycone and a terminal Rha at C-26 (residue III), while differ for the nature of the inner residue at C-26 (residue II) that is Gal for ceposide A and Glc for ceposide B. Ceposide C is a close analogue of ceposide A differing only for residue I that is Gal instead of Xyl. The comparable antifungal activity of ceposides A and C indicates that a change of the sugar residue at C-1 do not affect the activity. Therefore, the higher activity observed for ceposide B seems to be related to the presence of Glc

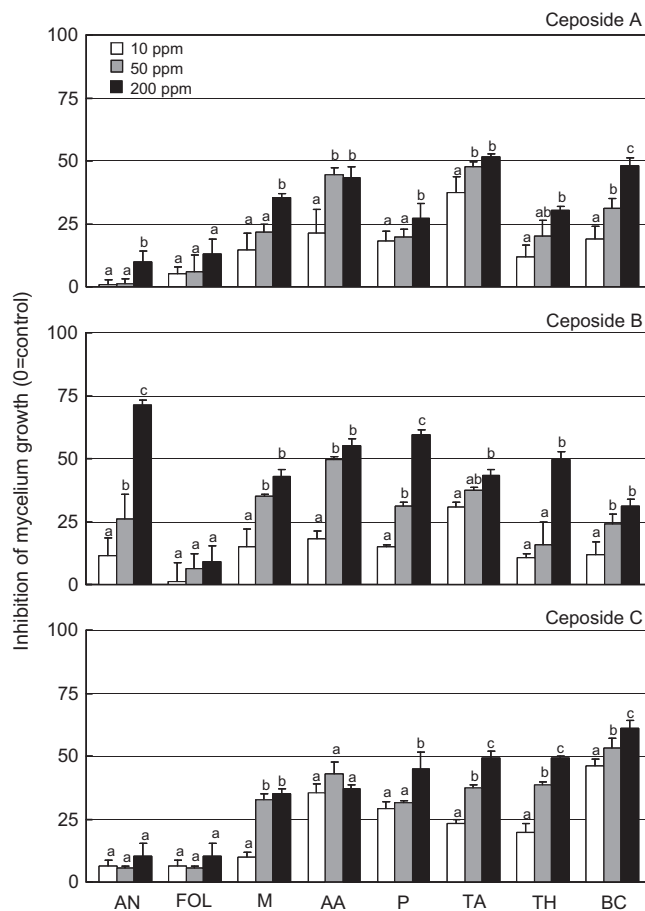


Fig. 2. Antifungal activity of three saponins isolated from *Allium cepa* at three concentrations (200, 50 and 10 p.p.m.). Data are inhibition of fungal growth in percentage compared to control (=0). Values are average of three replicates  $\pm$  standard deviation, different letters within each fungus indicate significant differences (Duncan test;  $P < 0.05$ ). Fungal acronyms as follow: AN = *Aspergillus niger*; FOL = *Fusarium oxysporum* f. sp. *lycopersici*; M = *Mucor* sp.; AA = *Alternaria alternata*; P = *Phomopsis* sp.; TA = *Trichoderma atroviride*; TH = *Trichoderma harzianum*; BC = *Botrytis cinerea*.

as inner residue at C-26. In detail, the new saponin cepeoside B showed a significant growth inhibition of all fungi with the exception of FOL, *Sclerotium cepivorum* and *Rhizoctonia solani* (Fig. 2). Cepeoside B was the only one capable to inhibit the growth of *A. niger* (Fig. 2). A previous study reported that triterpenoid saponins extracted from leaves of *Maesa lanceolata* were ineffective against this fungus (Sindambiwe et al., 1998). Cepeosides A and C were effective in reducing the growth of all fungi with the exception of *A. niger*, *S. cepivorum*, and FOL (Fig. 2). Concerning the growth of FOL, it was unaffected by all the three saponins, alone or in combination, even at their highest concentration (Fig. 2). This result contrasts with the FOL sensitivity to four of the five sapogenins and saponins extracted from *A. minutiflorum* (Barile, 2007). However, the active compounds are based on a spirostanol skeleton while cepeosides are based on a furostanol skeleton. Thus, their different FOL sensitivity could be related to the different nature of the aglycone. The lack of inhibitory effects of cepeosides on FOL could be due to capability of this fungus to detoxify such compounds. In fact, it is known that this pathogen of tomato (*Lycopersicon esculentum*) produces a tomatinase enzyme which hydrolyses the tomato glycoalkaloid  $\alpha$ -tomatine into less fungitoxic compounds (Roldán-Arjona et al., 1999). Further studies can explore the hypothesis the FOL is able to detoxify, in addition to  $\alpha$ -tomatine, also saponins based on a furostanol skeleton, such as cepeosides.

In the bioassays where saponins were applied in combination, additive effects (i.e. the inhibitory effect of mixed saponins was given by the sum of the single effects) were generally observed (data not shown). However, we found a significant synergism among the three saponins against *B. cinerea* and *Trichoderma atroviride* (Fig. 3). Growth of these two fungi was strongly inhibited when saponins were applied in combination, with *B. cinerea* showing a much larger inhibition at 10 and 50 p.p.m.

Consistently with a previous study carried out with saponins extracted from *A. minutiflorum* (Barile et al., 2007), the two *Trichoderma* species were very sensitive to the saponins (Fig. 2). Moreover, for *T. atroviride* we found a synergistic interaction between the three saponins, with a complete growth inhibition at 200 p.p.m. High sensitivity of *Trichoderma* species to saponins has been previously reported by Zimmer et al. (1967) and Nicol et al. (2002). The high sensitivity of *Trichoderma* species to saponins suggests that these compounds may act as chemical barriers that impede plant tissue colonization by such fungi. *Trichoderma* spp. are known to be able to infect roots but usually are not pathogenic to plants because they limit their infection to the superficial cell layer, thus inducing plant resistance responses (Harman et al., 2004).

Finally, the three saponins do not show appreciable antimicrobial activity, either alone or in combination, on *S. cepivorum* and *R. solani* (data not shown). A previous study (Abdel-Momen et al., 2000) reported that saponins extracted from a different plant, *Atri-*

*plex nummularia*, were effective in inhibiting the growth of *S. cepivorum*. Lack of cepeoside toxicity towards *S. cepivorum*, a specific pathogen of *Allium* species, and *R. solani*, a polyphagous soilborne pathogen, may be due to the ability of these fungi to degrade these saponins into non toxic molecules, thus allowing the attack to *A. cepa*. For instance, the fungus *G. graminis* var. *avenae* is able to infect oat plants because it produces avenacinase, an enzyme capable of detoxifying avenacins, the oat saponins (Bowyer et al., 1995). However, further studies are required to demonstrate the cepeoside detoxifying capability of *S. cepivorum* and *R. solani*.

### 3. Experimental

#### 3.1. General experimental procedures

Optical rotations were measured by a Perkin–Elmer 192 polarimeter equipped with a sodium lamp (589 nm) and 10-cm microcell. High-resolution ESIMS experiments were performed by an Applied Biosystem API 2000 triple-quadrupole mass spectrometer. The spectra were recorded by infusion into the ESI source using MeOH as solvent. GCMS analysis was performed by a Carlo Erba instrument. FTIR spectra were run on a Perkin–Elmer 1600 spectrometer in KBr.  $^1\text{H}$  and  $^{13}\text{C}$  NMR spectra were recorded by a Varian Unity Inova spectrometer at 500.13 and 125.77 MHz, respectively. Chemical shifts were referred to the residual solvent signal ( $\text{CD}_3\text{OD}$ :  $\delta_{\text{H}}$  3.31,  $\delta_{\text{C}}$  49.0). The multiplicities of  $^{13}\text{C}$  NMR resonances were determined by DEPT experiments.  $^1\text{H}$  connectivities were determined by COSY and HOHAHA experiments; the 2D HOHAHA experiments were performed in the phase-sensitive mode (TPPI) using the MLEV-17 (mixing time 125 ms) sequence for mixing. One-bond heteronuclear  $^1\text{H}$ – $^{13}\text{C}$  connectivities were determined with 2D HSQC pulse sequence with an interpulse delay set for  $^1\text{J}_{\text{CH}}$  of 130 Hz. Two and three bond heteronuclear  $^1\text{H}$ – $^{13}\text{C}$  connectivities were determined with 2D HMBC experiments, optimised for  $^{2-3}\text{J}_{\text{CH}}$  of 8 Hz. Nuclear Overhauser effect (NOE) measurements were performed by 2D ROESY experiments. Medium pressure liquid chromatography (MPLC) was performed in a Büchi 861 apparatus using LiChroprep RP-18 (40–63  $\mu\text{m}$ ) columns. Prep. TLC on  $\text{SiO}_2$  with  $\text{BuOH}:\text{H}_2\text{O}:\text{CH}_3\text{COOH}$  60:25:15 (BAW) for development was used. Spots were visualized with cerium sulphate in 2 N  $\text{H}_2\text{SO}_4$ . HPLC in isocratic mode was performed by a Varian apparatus equipped with a RI-3 refractive index detector [semipreparative  $\mu$ -Bondapack  $\text{C}_{18}$  column (7.8  $\times$  300 mm, i.d.)] and [analytical  $\mu$ -Bondapack  $\text{C}_{18}$  column (3.9  $\times$  300 mm, i.d.)].

#### 3.2. Plant material

Bulbs of white onion, *A. cepa* L., originating from Vesuvius area, near Naples, were bought in a market on March 2009. A voucher specimen (No. 0309) has been deposited at the Department of Food Science, University of Naples Federico II.

#### 3.3. Extraction and isolation

The bulbs (4.0 kg, fresh weigh) were finely chopped and exhaustively extracted with acetone four times using 2.5 L of solvent at room temperature, under stirring.

The acetone extract was taken to dryness and then partitioned between  $\text{EtOAc}$  and  $\text{H}_2\text{O}$  in order to solubilize lipids and apolar compounds in the organic layer. The watery layer was partitioned with  $\text{BuOH}$  in order to solubilize saponin compounds in the organic phase leaving sugars, aminoacids and salty compounds in the watery phase. The  $\text{BuOH}$  layer was filtered and then concentrated under vacuum giving a crude extract (22.3 g), which was chromatographed by MPLC on a RP-18 column using a linear gradient

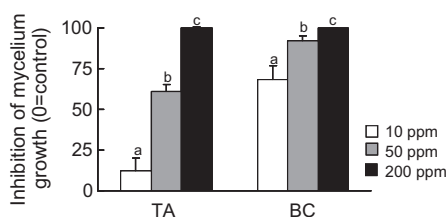


**Fig. 3.** Antifungal activity towards *Botrytis cinerea* (BC) and *Trichoderma atroviride* (TA) of three saponins isolated from *Allium cepa* and applied in even mixture (33% for each compound) at three final concentrations (200, 50 and 10 p.p.m.). Data are inhibition of fungal growth in percentage compared to control (=0). Values are average of three replicates  $\pm$  standard deviation, different letters within each fungus indicate significant differences (Duncan test;  $P < 0.05$ ).

solvent system from H<sub>2</sub>O to MeOH. Preliminary NMR study of the eluted fraction followed by TLC analyses (SiO<sub>2</sub>, butanol/acetic acid/water 60:15:25, v/v/v) revealed that only one fraction contained saponin compounds. This last fraction (72 mg, eluted with H<sub>2</sub>O–MeOH (1:1) was further purified by HPLC on a semipreparative C<sub>18</sub> column with the mobile phase H<sub>2</sub>O–MeOH (40:60), giving pure compound **1** (39.1 mg, *t*<sub>R</sub> = 3.2 min), ascalonicoside A (5.8 mg, *t*<sub>R</sub> = 4.3 min), and crude compounds **2** (12.1 mg, *t*<sub>R</sub> = 3.9 min) and **3** (8.3 mg, *t*<sub>R</sub> = 2.9 min). These latter compounds have been finally purified by HPLC on an analytical C<sub>18</sub> column with the mobile phase H<sub>2</sub>O–MeOH (40:60), giving respectively pure compounds **2** (10.2 mg) and **3** (6.8 mg).

#### 3.4. Ceposide A

(25R)-furost-5(6)-en-1β,3β,22α,26-tetraol 1-O-β-D-xylopyranosyl 26-O-α-D-rhamnopyranosyl-(1 → 2)-O-β-D-galactopyranoside (**1**); Yield: 39.1 mg; colorless amorphous solid;  $[\alpha]_D^{25} -30.7^\circ$  (*c* = 0.1 MeOH); IR (KBr)  $\nu_{\max}$  3410, 2930, 1150 and 1045 cm<sup>-1</sup>; <sup>1</sup>H NMR data, see Tables 1 and 3; <sup>13</sup>C NMR data, see Table 2. HRFABMS (negative ion): found *m/z* 887.4632 [M–H]<sup>-</sup>; calculated for C<sub>44</sub>H<sub>71</sub>O<sub>18</sub> *m/z* 887.4647.

#### 3.5. Ceposide B

(25R)-furost-5(6)-en-1β,3β,22α,26-tetraol 1-O-β-D-xylopyranosyl 26-O-α-D-rhamnopyranosyl-(1 → 2)-O-β-D-glucopyranoside (**2**); Yield: 10.2 mg; colorless amorphous solid;  $[\alpha]_D^{25} -35.2^\circ$  (*c* = 0.1 MeOH); IR (KBr)  $\nu_{\max}$  3413, 2932, 1150 and 1043 cm<sup>-1</sup>; <sup>1</sup>H NMR data, see Tables 1 and 3; <sup>13</sup>C NMR data, see Table 2. HRFABMS (negative ion): found *m/z* 887.4628 [M–H]<sup>-</sup>; calculated for C<sub>44</sub>H<sub>71</sub>O<sub>18</sub> *m/z* 887.4647.

#### 3.6. Ceposide C

(25R)-furost-5(6)-en-1β,3β,22α,26-tetraol 1-O-β-D-galactopyranosyl 26-O-α-D-rhamnopyranosyl-(1 → 2)-O-β-D-galactopyranoside (**3**); Yield: 6.8 mg, colorless amorphous solid;  $[\alpha]_D^{25} -41.7^\circ$  (*c* = 0.1 MeOH); IR (KBr)  $\nu_{\max}$  3400, 2934, 1159 and 1048 cm<sup>-1</sup>; <sup>1</sup>H NMR data, see Tables 1 and 3; <sup>13</sup>C NMR data, see Table 2. HRFABMS (negative ion): found *m/z* 917.4715 [M–H]<sup>-</sup>; calculated for C<sub>45</sub>H<sub>73</sub>O<sub>19</sub> *m/z* 917.4726.

#### 3.7. Determination of sugar absolute configurations

A solution of each isolated compound (1 mg) in 1 N HCl (0.25 ml) was stirred at 80 °C for 4 h. While cooling, the solution was concentrated under a stream of N<sub>2</sub>. The residue was dissolved in 1-(trimethyl silyl)imidazole (Trisil-Z) and pyridine (0.1 ml) and the solution was stirred at 60 °C for 5 min. The solution was dried with a stream of N<sub>2</sub>, and the residue was separated by water and CH<sub>2</sub>Cl<sub>2</sub> (1 mL, 1:1). The CH<sub>2</sub>Cl<sub>2</sub> layer was analyzed by GC (Alltech I-Chirasil-Val column, 0.32 × 25 m; temperatures for injector and detector, 200 °C; temperature gradient system for the oven, 100 °C for 1 min and then raised to 180 °C; rate 5 °C/min). Peaks of the hydrolysate of **1** were detected at 10.98, 12.89, and 13.98 min in the ratio of 1:1:1. Peaks of the hydrolysate of **2** were detected at 10.98, 12.89, and 14.66 min in the ratio of 1:1:1. Peaks of the hydrolysate of **3** were detected at 12.89 and 13.98 min in the ratio of 1:2. Retention times for authentic samples after being treated simultaneously with Trisil-Z were 10.98 (D-xylose) and 11.05 (L-xylose), 12.78 (D-rhamnose) and 12.89 (L-rhamnose), 13.98 (D-galactose) and 13.75 (L-galactose), 14.66 (D-glucose) and 14.73 min (L-glucose). Co-injection with standard D-xylose, D-galactose, and L-rhamnose for the hydrolysate of **1**, with standard D-xylose, D-glucose, and L-rhamnose for the hydrolysate of **2**, with

standard D-galactose and L-rhamnose for the hydrolysate of **3** gave single peaks.

#### 3.8. Biological assays

Antifungal activity of the three ceposides was tested on 10 different fungal species. Three soil-borne pathogens (*Fusarium oxysporum* f. sp. *lycopersici*, *R. solani* and *Sclerotium cepivorum*), five air-borne pathogens (*Alternaria alternata*, *Aspergillus niger*, *B. cinerea*, *Mucor* sp., *Phomopsis* sp.) and two antagonistic fungi (*T. atroviride* and *Trichoderma harzianum*) were selected. *S. cepivorum* was used because is a pathogen specific of the *Allium* genus. All microbes were obtained from Department of Arboriculture, Botany and Plant pathology, Agriculture Faculty (NA), Italy. Antifungal activity was assessed by in vitro test following Barile et al. (2006). Briefly, a suspension of 10<sup>3</sup> spores was prepared in 50 μl of 0.1 strength PDB with 15 μl of 5 mM potassium phosphate buffer (pH 6.7). Saponins were added at three concentrations (200, 50 and 10 p.p.m.) in a 96-well plate and incubated at 25 °C. Fungal hyphal length of germinating spore was measured after 14 to 24 h depending on the fungal species. For *Rhizoctonia* and *S. cepivorum* the antifungal activity was evaluated with a petri dish growth assay because such microbes do not produce conidia. Plates of 9 cm of PDA added with the saponins at three concentrations as above described, were inoculated with a 5 mm plug containing the fungi. Plates were incubated at 25 °C and the fungi radial growth was measured after 24, 48 and 72 h. Finally, antifungal synergistic effects of the three saponins were assessed on all fungi, by applying the compounds in even mixtures (33% for each one) at three final concentrations (200, 50 and 10 p.p.m.). Inhibition of fungal growth was statistically evaluated by one-way ANOVA by using molecule concentrations as a factor for each fungus. Significance was evaluated in all cases at *P* < 0.05 and *P* < 0.01.

#### Acknowledgements

Mass and NMR spectra were recorded at CSIAS, University of Naples Federico II. The assistance of the staff is gratefully acknowledged. We also thank Alessandra Gargiulo and Vincenzo Antignani for technical assistance in laboratory analyses.

#### References

- Abdel-Momen, S.M., Omar, S.A., Hanafi, A.A., Abdel-Rahman, T.M., 2000. Different sources of saponin affecting white rot disease in onion (*Allium cepae* L.). Bulletin of Faculty of Agriculture, University of Cairo 51, 365–377.
- Barile, E., Bonanomi, G., Antignani, V., Zolfaghari, B., Ebrahim Sajjadi, S., Scala, F., Lanzotti, V., 2007. Saponins from *Allium minutiflorum* with antifungal activity. Phytochemistry 68, 596–603.
- Bowyer, P., Clarke, B.R., Lunness, P., Daniels, M.J., Osbourn, A.E., 1995. Host range of a plant pathogenic fungus determined by a saponin detoxifying enzyme. Science 267, 371–374.
- Corea, G., Fattorusso, E., Lanzotti, V., Capasso, R., Izzo, A.A., 2005. Antospasmodic Saponins from Bulbs of Red Onion, *Allium cepa* L. Var. Tropea. J. Nat. Prod. 66, 1405–1411.
- Corea, G., Fattorusso, E., Lanzotti, V., 2003. Saponins and flavonoids of *Allium triquetrum*. J. Nat. Prod. 66, 1405–1411.
- De Lucca, A.J., Bland, J.M., Boue, S., Vigo, C.B., Cleveland, T.E., Walsh, T.J., 2006. Synergism of CAY-1 with Amphotericin B and Itraconazole. Chemotherapy 52, 285–287.
- Dixon, R.A., 2001. Natural products and plant disease resistance. Nature 411, 843–847.
- Dong, M., Feng, X., Wang, B., Wu, L., Ikejima, T., 2001. Two novel furostanol saponins from the rhizomes of *Dioscorea panthaica* Prain et Burkill and their cytotoxic activity. Tetrahedron 57, 501–506.
- Fattorusso, E., Iorizzi, M., Lanzotti, V., Tagliatalata Scafati, O., 2002. Chemical composition of shallot (*Allium ascalonicum* Hort.). J. Agr. Food Chem. 50, 5686–5690.
- Harmann, G.E., Howell, C.R., Viterbo, A., Chet, I., Lorito, M., 2004. *Trichoderma* species-opportunistic, avirulent plants symbionts. Nat. Rev. 2, 43–56.
- Lanzotti, V., 2006. The analysis of onion and garlic. J. Chromat. A 1112, 3–22.
- Lanzotti, V., 2005. Bioactive Saponins from *Allium* and *Aster* plants. Phytochem. Rev. 4, 95–110.

- Lorito, M., Peterbauer, C., Hayes, C.K., Harman, G.E., 1994. Synergistic interaction between fungal cell wall degrading enzymes and different antifungal compounds enhances inhibition of spore germination. *Microbiology* 140, 623–629.
- Morrissey, J.P., Osbourn, A.E., 1999. Fungal resistance to plant antibiotics as a mechanism of pathogenesis. *Micribiol. Mol. Biol. Rev.* 63, 708–724.
- Nicol, R.W., Traquair, J.A., Bernards, M.A., 2002. Ginsenosides as host resistance factors in American ginseng (*Panax quinquefolius*). *Can. J. Bot.* 80, 557–562.
- Osbourn, A.E., 1996. Saponins and plant defence - a soap story. *Trends Plant Sci.* 1, 4–9.
- Roldán-Arjona, T., Pérez-Espinosa, A., Ruiz-Rubio, M., 1999. Tomatinase from *Fusarium oxysporum* f. sp. *lycopersici* defines a new class of saponinases. *Mol. Plant Microbe Interact.* 12, 852–861.
- Segura, A., Moreno, M., Madueno, F., Molina, A., Garcia-Olmedo, F., 1999. Snakin-1, a peptide from potato that is active against plant pathogens. *Mol. Plant Microbe Interact.* 12, 16–23.
- Sindambiwe, J.B., Calomme, M., Geerts, S., Pieters, L., Vlietinck, A.J., Vanden Berghe, D.A., 1998. Evaluation of biological activities of triterpenoid saponins from *Maesa lanceolata*. *J. Nat. Prod.* 61, 585–590.
- VanEtten, H.D., Mansfield, J.W., Bailey, J.A., Farmer, E.E., 1994. Two classes of plant antibiotics: Phytoalexins versus “phytoanticipins”. *Plant Cell* 9, 1191–1192.
- Wittstock, U., Gershenzon, J., 2002. Constitutive plant toxins and their role in defense against herbivores and pathogens. *Curr. Opin. Plant Biol.* 5, 1–8.
- Zimmer, D.E., Pedersen, M.W., McGuire, D.F., 1967. A bioassay for alfalfa saponins using the fungus *Trichoderma viride*. *Pers. ex. Fr. Crop. Sci.* 7, 223–224.